

# Neural Operators for Predictor Feedback Control of Nonlinear Delay Systems

**Luke Bhan\***

*University of California, San Diego*

LBHAN@UCSD.EDU

**Peijia Qin\***

*University of California, San Diego  
Southern University of Science and Technology*

PQIN@UCSD.EDU

**Miroslav Krstic**

*University of California, San Diego*

MKRSTIC@UCSD.EDU

**Yuanyuan Shi**

*University of California, San Diego*

YYSHI@UCSD.EDU

## Abstract

Predictor feedback designs are critical for delay-compensating controllers in nonlinear systems. However, these designs are limited in practical applications as predictors cannot be directly implemented, but require numerical approximation schemes. These numerical schemes, typically combining finite difference and successive approximations, become computationally prohibitive when the dynamics of the system are expensive to compute. To alleviate this issue, we propose approximating the predictor mapping via a neural operator. In particular, we introduce a new perspective on predictor designs by recasting the predictor formulation as an operator learning problem. We then prove the existence of an arbitrarily accurate neural operator approximation of the predictor operator. Under the approximated-predictor, we achieve semiglobal practical stability of the closed-loop nonlinear system. The estimate is semiglobal in a unique sense - namely, one can increase the set of initial states as large as desired but this will naturally increase the difficulty of training a neural operator approximation which appears practically in the stability estimate. Furthermore, we emphasize that our result holds not just for neural operators, but any black-box predictor satisfying a universal approximation error bound. From a computational perspective, the advantage of the neural operator approach is clear as it requires training once, offline and then is deployed with very little computational cost in the feedback controller. We conduct experiments controlling a 5-link robotic manipulator with different state-of-the-art neural operator architectures demonstrating speedups on the magnitude of  $10^2$  compared to traditional predictor approximation schemes.

**Keywords:** Neural operators, Nonlinear systems, Delay systems, Predictor feedback

## 1. Introduction

Modern applications such as telerobotics (Lum et al., 2009; Abadía et al., 2021), renewable energy based power-systems (Magnússon et al., 2020), biomedical devices (Sharma et al., 2011) and unmanned vehicles (Wang et al., 2020; Mazenc et al., 2022) all suffer from communication, sensor, and network delays that are critical to performance. Therefore, in order to deploy functional and real-world controllers, engineers need to design proactive, delay compensating control laws. Given this, dynamical systems under delays have been a consistent focal point for control design since the

---

\* Equal contribution

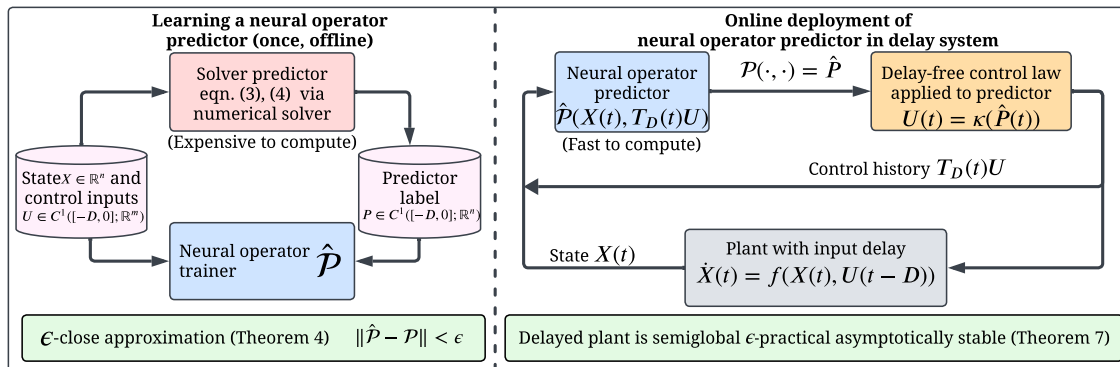


Figure 1: Overview of learning neural operator predictors for compensating delays in nonlinear systems.

introduction of the Smith predictor in 1957 (Smith, 1957; Henson and Seborg, 1994; Kravaris and Wright, 1989; Jankovic, 2001, 2003; Mazenc and Bliman, 2003; Karafyllis, 2006).

In this work, we focus on predictor feedback controllers (Artstein, 1982; Kwon and Pearson, 1980). Predictor feedback designs mitigate delays by deploying the delay-free control law with not the system’s current state, but a *prediction of the system’s future state*. This approach have been developed for both linear (Zhou, 2014; Jankovic, 2010; Cacace and Germani, 2017) and nonlinear systems including state-dependent delays (Bekiaris-Liberis and Krstic, 2011), delay-adaptive control (Bresch-Pietri and Krstic, 2014), multi-input delay control (Bekiaris-Liberis and Krstic, 2017). However, the nonlinear predictor feedback designs are limited, as the explicit predictor feedback mappings are rarely available for implementation (Bekiaris-Liberis and Krstic, 2013). To address this, engineers approximate the predictor mapping with numerical schemes such as successive approximations (Karafyllis and Krstic, 2017, Chapter 4). Unfortunately, these approaches suffer when the dynamics of the system are expensive to compute.

In this work, we introduce a new class of predictor feedback design with neural approximated predictors that are both theoretically stable and real-world computationally efficient. Specifically, we recast the predictor mapping as a *mathematical operator*, and propose learning a neural operator (NeuralOP) approximation of it (Figure 1 left). From a theoretical standpoint, we prove the continuity of the predictor operator, thus guaranteeing the existence of a NeuralOP that can approximate the original operator to any desired accuracy. From a computational perspective, we inherit the excellent speedups and scalability (with respect to discretization sizes) of NeuralOPs (Li et al., 2021; Lu et al., 2021), which has been highlighted across a series of control designs including gain-scheduling (Lamarque et al., 2024b), adaptive control (Bhan et al., 2024, 2025; Lamarque et al., 2024a), traffic flows (Zhang et al., 2024; Lv et al., 2024), and PDE boundary control under delays (Qi et al., 2024).

To analyze the proposed predictor feedback design in closed-loop systems (Figure 1 right), we present a new analytical framework for studying nonlinear delay systems with black-box approximations of predictors. We showcase, that under uniform approximation error bounds, the resulting delay system achieves *semiglobal practical stability* (dependent on the approximation error). In our analysis, we rely on a transport PDE representation of the delay which, when coupled with an infinite dimensional backstepping transformation, yields a perturbed system that is shown to be arbitrarily stable based on the approximation error. A key advantage of our analysis is that it applies

to any *black-box predictor* satisfying a universal approximation error bound. As such, predictor approximation techniques beyond NeuralOPs, such as Neural ordinary differential equations (Neural ODEs) (Chen et al., 2018), recurrent neural networks (RNNs) (Cho et al., 2014; Aguiar et al., 2024), and generative models (Chen and Xiu, 2024) all apply under our theoretical analysis. Lastly, to highlight the computational speedups of our approach, we consider predictor feedback control on a challenging 5-link robotic manipulator as in Bagheri et al. (2019). On such a problem, comparing across a variety of deep learning architectures, we showcase speedups of  $10^2$  magnitude over the numerical approximations in Karafyllis and Krstic (2017) while still maintaining stability.

**Notation** For functions,  $f : [0, D] \times \mathbb{R} \rightarrow \mathbb{R}$ , we use the PDE notation  $f_x(x, t) = \frac{\partial f}{\partial x}(x, t)$  and similarly  $f_t(x, t) = \frac{\partial f}{\partial t}(x, t)$  to denote derivatives. We use  $C^1([t - D, t]; \mathbb{R}^m)$  to denote the set of functions with continuous first derivatives mapping the interval  $[t - D, t]$  to  $\mathbb{R}^m$ . Further, we use the notation  $T_D(t)f$  to indicate the set  $\{f(t + \theta); \theta \in [-D, 0]\}$  which represents the evaluation of the function  $f$  with inputs from  $[t - D, t]$ . For a  $n$ -vector we use  $|\cdot|$  for the Euclidean norm. For functions, we define the spatial  $L^p$  norms as  $\|f(t)\|_{L^p[0, D]} = (\int_0^D |f(x, t)|^p dx)^{\frac{1}{p}}$  for  $p \in [1, \infty)$ . We use  $\|f(t)\|_{L^\infty[0, D]} = \sup_{0 \leq x \leq D} |u(x, t)|$  to denote the spatial  $L^\infty$  norm.

## 2. Preliminaries: Exact Predictor Feedback Designs for Nonlinear Delay Systems

In this work, we consider nonlinear systems with input delay of the form

$$\dot{X}(t) = f(X(t), U(t - D)), \quad (1)$$

where  $X \in \mathbb{R}^n$  is the state vector,  $U \in \mathbb{R}^m$  is the control,  $f : \mathbb{R}^n \times \mathbb{R}^m \rightarrow \mathbb{R}^n$  represents the system dynamics and  $D \in [0, \infty)$  is a constant, known delay. The classic predictor-feedback design consists of two components, namely a predictor, which we denote  $P(t)$ , and the nominal, delay-free control law  $\kappa(X(t))$ . The delay-compensating control law then becomes

$$U(t) = \kappa(P(t)), \quad (2)$$

$$P(t) = \int_{t-D}^t f(P(\theta), U(\theta)) d\theta + X(t), \quad (3)$$

where the initial condition for the integral equation is given by

$$P(\theta) = \int_{-D}^{\theta} f(P(\sigma), U(\sigma)) d\sigma + X(0), \quad \theta \in [-D, 0]. \quad (4)$$

In essence, the predictor feedback  $P(t)$ , implicitly defined in (3), (4) is the  $D$ -second ahead prediction of the state, i.e.  $P(t) = X(t + D)$ . For pedagogical organization as well as clarity, we now briefly review the stability analysis for the *exact* control law (2), (3), (4) from Krstic (2010) highlighting the type of guarantees that we aim to attain under the proposed neural operator approximated predictor. To do so, we require the following assumptions.

**Assumption 1**  $\dot{X} = f(X, \omega)$  in (1) is strongly forward complete. (See Appendix A.1 for definition).

**Assumption 2** The system  $\dot{X} = f(X, \kappa(X) + \omega)$  in (1) is input-to-state stable (ISS). (See Appendix A.2 for ISS definition).

Both assumptions are standard in the predictor-feedback literature (Bekiaris-Liberis and Krstic, 2013). Forward-completeness is needed to ensure the predictor system does not exhibit finite escape time and we use ISS to explicitly to construct the Lyapunov functional. Lastly, we assume the existence of a globally asymptotically stabilizing control law for the system *without delays*.

**Assumption 3** *There exists a control law  $U(t) = \kappa(X(t))$  such that the delay-free system  $\dot{X}(t) = f(X(t), U(t))$  is globally asymptotically stable.*

Assumption 3 ensures the delay-free controller is globally asymptotically stable, but can be relaxed with the expectation that the stability result for the predictor feedback controller correspondingly weakens. We now present the stability result under the exact predictor feedback.

**Theorem 1** (Krstic, 2010, Theorem 11) *Let Assumptions 1, 2, 3 hold for (1). Then, with the controller (2), (3) for all  $t \geq 0$ , there exists  $\beta_1 \in \mathcal{KL}$  such that*

$$|X(t)| + \sup_{t-D \leq \tau \leq t} |U(\tau)| \leq \beta_1 \left( |X(0)| + \sup_{-D \leq \tau \leq 0} |U(\tau)|, t \right). \quad (5)$$

To obtain Theorem 1, a crucial ingredient in the stability analysis is to represent the input delay in the system dynamics (1) as a *transport PDE*, coupled with the nonlinear ODE plant model,

$$\dot{X}(t) = f(X(t), u(t, 0)), \quad t \in [0, \infty), \quad (6a)$$

$$u_t(x, t) = u_x(x, t), \quad (x, t) \in [0, D] \times [0, \infty), \quad (6b)$$

$$u(D, t) = \kappa(P(t)), \quad t \in [0, \infty). \quad (6c)$$

where the predictor in PDE notation becomes  $P(t) = p(D, t)$  with

$$p(x, t) = \int_0^x f(p(\xi, t), u(\xi, t)) d\xi + X(t), \quad (x, t) \in [0, D] \times [0, \infty). \quad (7)$$

Notice that, although we have introduced a second variable  $x$ , the predictor (7) is equivalent to (3) and thus is still defined implicitly as the solution to an *ODE*, namely

$$p_x(x, t) = f(p(x, t), u(x, t)), \quad p(0, t) = X(t), \quad (8)$$

where  $p(x, t) = P((t-D) + x)$ . The core idea of rewriting (1) as (6a), (6b), (6c) is that the delayed input  $U(t-D)$  is now represented via the transport PDE (6b), (6c) allowing one to analyze the nonlinear delay system via a coupled ODE-PDE system. However, the boundary condition in (6c) is unbounded and thus hinders the stability analysis of the coupled system. To abate this issue, we introduce the following infinite dimensional *backstepping transformation* which transforms  $u(x, t)$  into what we call the *target system*  $w(x, t)$ .

$$w(x, t) = u(x, t) - \kappa(p(x, t)), \quad (9)$$

$$u(x, t) = w(x, t) + \kappa(\pi(x, t)), \quad (10)$$

where  $\pi(x, t)$  satisfies

$$\pi(x, t) = \int_0^x f(\pi(\xi, t), \kappa(\pi(\xi, t)) + w(\xi, t)) d\xi + X(t). \quad (11)$$

First, note that, by definition  $\pi(x, t) = p(x, t)$ , but is rewritten in terms of the  $w$  variables whereas  $p(x, t)$  is written in terms of the  $u$  variable in (7). Second, note that the transformation between  $w$  and  $u$  is invertible, and therefore, analysis conducted on the  $w$  system will correspondingly apply to the  $u$  system. Third, under the transformation (9), (10), we obtain the following target system,

$$\dot{X}(t) = f(X(t), \kappa(X(t)) + w(t, 0)), \quad t \in [0, \infty), \quad (12a)$$

$$w_t(x, t) = w_x(x, t), \quad (x, t) \in [0, D) \times [0, \infty), \quad (12b)$$

$$w(D, t) = 0, \quad t \in [0, \infty). \quad (12c)$$

The target system highlights the key advantage of the backstepping transformation as we now see the removal of the boundary condition in (12c) compared to (6c). Thus, it is feasible to show that the  $w$  transport PDE is globally exponentially stable in the  $L^\infty$  norm (In fact, it is finite-time stable). From here, one can combine the stability of the  $w$  PDE with the ISS property of  $X$ , obtaining a bound on the coupled ODE-PDE system. To complete the result of Theorem 1, one invokes the invertibility of the backstepping transformation to transform the estimate in the  $X$  and  $w$  system back into an estimate on the  $X$  and  $u$  system.

Although the exact predictor feedback achieves global asymptotic stability as in Theorem 1, the explicit solution of the nonlinear system is rarely available, and therefore the predictor is almost never implementable exactly. Thus, numerical schemes such as the successive approximations in Karafyllis and Krstic (2017) need to be employed, but these become computationally intractable when the system is stiff or has long input delays. Due to these limitations, in this work, we pursue NeuralOP approximation of predictor that is both implementable and retains stability guarantees.

### 3. Stability under NeuralOP Approximated Predictor Feedback

We present our main framework for delay-compensating feedback controllers under approximate predictors. In Section 3.1, we formulate the predictor approximation as an *operator learning problem* and prove the existence of arbitrarily close NeuralOP based approximations to the predictor. Then, in Section 3.2, we analyze the resulting target system  $w$  under the approximate predictor. We develop a  $L^\infty$  estimate of the *perturbed* transport PDE where the perturbation is directly due to the approximation error. Lastly, we use the stability estimates of this perturbed PDE to analyze the coupled ODE-PDE system, proving semiglobal practical stability of the closed-loop system.

#### 3.1. Approximation of the predictor operator via NeuralOP

We begin by first defining the predictor operator as the solution to the ODE (3), (4) and proving existence of a uniform NeuralOP based approximation. Naturally, we will let the predictor operator be the mapping from  $X(t)$  and the history of the costs  $T_D(t)U := \{U(t + \theta); \theta \in [-D, 0]\}$  into the solution to the predictor ODE (3), (4).

**Definition 2 (Predictor operator)** Let  $X \in \mathbb{R}^n$ ,  $U \in C^1([-D, 0]; \mathbb{R}^m)$ . Then, we define the predictor operator mapping as  $\mathcal{P} : (X, U) \rightarrow P$  where  $\mathcal{P}$  maps from  $\mathbb{R}^n \times C^1([-D, 0]; \mathbb{R}^m)$  to  $C^1([-D, 0]; \mathbb{R}^n)$  and where  $P(s) = \mathcal{P}(X, U)(s)$  satisfies for all  $s \in [-D, 0]$ ,

$$P(s) - \int_{-D}^s f(P(\theta), U(\theta))d\theta - X = 0, \quad s \in [-D, 0]. \quad (13)$$

We aim to show that for any desired accuracy  $\epsilon > 0$ , there exists a NeuralOP approximation to the predictor operator  $\mathcal{P}$ . To do so, we require the assumption of global Lipschitz dynamics.

**Assumption 4** *Let  $f(X, U)$  as in (1). Then, there exists a constant  $C_f > 0$  such that  $f$  satisfies the Lipschitz condition*

$$|f(x_1, u_1) - f(x_2, u_2)| \leq C_f(|x_1 - x_2| + |u_1 - u_2|), \quad (14)$$

for all  $x_1, x_2 \in \mathbb{R}^n$  and  $u_1, u_2 \in \mathbb{R}^m$ .

Assumption 4, although strong, is necessary to ensure the global continuity of the predictor and is similarly needed in numerical approximation schemes such as finite difference and successive approximations (Karafyllis and Krstic, 2017).

To invoke the universal operator approximation theorem in Lanthaler et al. (2023) (summarized in Appendix A.4), we first establish the continuity of the predictor  $\mathcal{P}$  in the following Lemma.

**Lemma 3** *Let Assumption 4 hold. Then, for any  $X_1, X_2 \in \mathbb{R}^n$  and control functions  $U_1, U_2 \in C^1([-D, 0]; \mathbb{R}^m)$ , the predictor operator  $\mathcal{P}$  defined in (13) satisfies*

$$\|\mathcal{P}(X_1, U_1) - \mathcal{P}(X_2, U_2)\|_{L^\infty([-D, 0])} \leq C_{\mathcal{P}} (|X_1 - X_2| + \|U_1 - U_2\|_{L^\infty([-D, 0])}), \quad (15)$$

with Lipschitz constant

$$C_{\mathcal{P}} := \max(1, DC_f)e^{DC_f}, \quad (16)$$

where  $D$  is the delay constant and  $C_f$  is the system Lipschitz constant defined in Assumption 4.

Applying the continuity of  $\mathcal{P}$  with the universal approximation theorem of neural operators (detailed in Appendix A.4) yields

**Theorem 4** *Let  $X \in \mathcal{X} \subset \mathbb{R}^n$  and  $U \in C^1([-D, 0]; \mathcal{U})$  where  $\mathcal{U} \subset \mathbb{R}^m$  is a bounded domain. Fix a compact set  $K \subset \mathcal{X} \times C^1([-D, 0]; \mathcal{U})$ . Then, for all  $\bar{X}, \bar{U}, \epsilon > 0$ , there exists a neural operator approximation  $\hat{\mathcal{P}} : K \rightarrow C^1([-D, 0]; \mathbb{R}^n)$  such that*

$$\sup_{(X, U) \in K} |\mathcal{P}(X, U)(\theta) - \hat{\mathcal{P}}(X, U)(\theta)| < \epsilon, \quad \forall \theta \in [-D, 0], \quad (17)$$

for all  $X \in \mathcal{X}$ ,  $U \in C^1([-D, 0]; \mathcal{U})$  such that  $|X| < \bar{X}$  and  $\|U\|_{L^\infty([-D, 0])} < \bar{U}$ .

First, notice that Theorem 4 requires a compact domain of functions and thus restricts the possibility of global stability guarantees. This type of compactness similarly appears in Bhan et al. (2024, Section VI) and is a common restriction of almost all universal approximation theorems. Further, Theorem 4 guarantees the *existence* of a neural operator approximation, but does not provide a minimum number of network parameters nor data samples to achieve such errors. To obtain practical estimates - which are architecture dependent - we refer the reader to Lanthaler et al. (2022) and Kovachki et al. (2021) whose results can be directly applied in conjunction with Theorem 4.

### 3.2. Perturbed Transport PDE under the approximated predictor

We now focus on analyzing the resulting stability properties of the system with the approximate predictor. For notational simplicity, define  $\hat{P}$  as the solution to the operator approximation, namely

$$\hat{P}(t) = \hat{\mathcal{P}}(X(t), T_D(t)U), \quad \forall t \geq 0. \quad (18)$$

where  $P(t)$  is now the predictor operator mapping defined in (13) applied to the solution  $X(t)$  and the historical control input from  $[t - D, t)$ . Under the approximation, the system becomes

$$\dot{X}(t) = f(X(t), u(t, 0)), \quad t \in [0, \infty), \quad (19a)$$

$$u_t(x, t) = u_x(x, t), \quad (x, t) \in [0, D) \times [0, \infty), \quad (19b)$$

$$u(D, t) = \kappa(\hat{P}(t)), \quad t \in [0, \infty). \quad (19c)$$

where (19c) differs from (6c) as we invoke the controller with the approximate predictor. Applying the backstepping transform results in the following target system.

**Lemma 5** *The system (19b), (19a), (19c) under the backstepping transformation (9), (10) becomes,*

$$\dot{X}(t) = f(X(t), \kappa(X(t)) + w(t, 0)), \quad t \in [0, \infty), \quad (20a)$$

$$w_t(x, t) = w_x(x, t), \quad (x, t) \in [0, D) \times [0, \infty), \quad (20b)$$

$$w(D, t) = \kappa(P(t)) - \kappa(\hat{P}(t)), \quad t \in [0, \infty). \quad (20c)$$

The key challenge is that (20c) now contains a non-vanishing, but arbitrarily small perturbation depending on the prediction error between  $P$  and the operator approximation  $\hat{P}$ . As such, we introduce the following Lemma for characterizing the exact  $L^\infty$  stability properties of the perturbed  $w$  transport PDE under the predictor approximation error.

**Lemma 6** *(ISS estimate for  $L^\infty$  norm of perturbed transport PDE) Let  $c > 0$  be a constant. Then, the transport PDE (20b), (20c) satisfies, for all  $t \geq 0$ , the following ISS-like stability estimate*

$$\|w(t)\|_{L^\infty[0, D]} \leq e^{c(D-t)} \|w(0)\|_{L^\infty[0, D]} + e^{cD} \sup_{0 \leq s \leq t} |\kappa(P(t)) - \kappa(\hat{P}(t))|. \quad (21)$$

Notice that Lemma 6 does not guarantee asymptotic stability of  $w$  to the equilibrium 0, but instead to a set depending on the maximum difference between the predictor and its approximator which is uniformly bounded by  $\epsilon$  - hence the system is globally asymptotically practically stable in  $\epsilon$ .

### 3.3. Stability of the delay system under NeuralOP approximated predictor feedback

Following Lemma 6, we have now arrived at a bound on the target PDE (20b), (20c) under the approximated predictor. All that remains is to combine Lemma 6 with the coupled ODE system and the inverse backstepping transform (10). After a series of calculations detailed in Appendix B.5, we arrive at the following main result.

**Theorem 7** *Let the system (20a), (20b), (20c) satisfy Assumptions 1, 2, 4 and assume that  $\kappa$  is stabilizing as in Assumption 3. Then, for  $\bar{\mathcal{B}} := \bar{\mathcal{X}} + \bar{\mathcal{U}}$ , there exists functions  $\alpha_1 \in \mathcal{K}$  and  $\beta_2 \in \mathcal{KL}$  such that if  $\epsilon < \epsilon^*$  where*

$$\epsilon^*(\bar{\mathcal{B}}) := \alpha_1^{-1}(\bar{\mathcal{B}}), \quad (22)$$

and the initial state is constrained to

$$|X(0)| + \sup_{-D \leq \theta \leq 0} |U(\theta)| \leq \Omega, \quad (23)$$

where

$$\Omega(\epsilon, \bar{\mathcal{B}}) := \bar{\alpha}_2^{-1}(\bar{\mathcal{B}} - \alpha_1(\epsilon)), \quad \bar{\alpha}_2(r) = \beta_2(r, 0), \quad r \geq 0, \quad (24)$$

then, the closed-loop solutions, under the controller with the neural operator-approximated predictor  $U(t) = \kappa(\hat{P}(t))$ , satisfy the  $\bar{\mathcal{B}}$ -semiglobal and  $\epsilon$ -practical stability estimate

$$|X(t)| + \sup_{t-D \leq \theta \leq t} |U(\theta)| \leq \beta_2 \left( |X(0)| + \sup_{-D \leq \theta \leq 0} |U(\theta)|, t \right) + \alpha_1(\epsilon), \quad \forall t \geq 0, \quad (25)$$

with the neural operator semiglobally trained with  $\bar{\mathcal{B}} > \bar{\alpha}_2(\Omega)$  and  $\epsilon \in (0, \alpha_1^{-1}(\bar{\mathcal{B}}))$ .

Note, as aligned with the semiglobal property, the radius of initial conditions  $\Omega$  can be made arbitrarily large given that one increases  $\bar{\mathcal{B}}$ . However, one will then pay a price as the neural operator will be harder to train to the desired  $\epsilon$  for a larger set of  $\bar{\mathcal{B}}$ . Thus, practically, one will need a larger training set and more neurons in the architecture to achieve the same  $\epsilon$  when increasing  $\bar{\mathcal{B}}$ . Additionally, it may be counter intuitive that  $\epsilon^*$  grows with  $\bar{\mathcal{B}}$ , but the reader will recognize that a larger set of system states permits a larger transient and therefore a coarser approximation of the predictor. However, despite the larger tolerance in  $\epsilon^*$ , it is undesirable to have a large  $\epsilon$  due to the fact the stability estimate is  $\epsilon$ -practical in (25). Lastly, note in the case of perfect approximation, i.e.  $\epsilon = 0$ , we recover the result of Theorem 1.

We briefly comment on the result of Theorem 7 compared to those of Karafyllis and Krstic (2017, Theorem 5.1 and Theorem 5.3). Both results of Karafyllis and Krstic (2017) obtain global asymptotic and local exponential stability, but require system dependent-assumptions on either the predictor implementation or the growth rate of the dynamics in order to annihilate the approximation error. In contrast, our result makes no assumption of the approximation scheme relying only on an uniform  $\epsilon$  bound of the predictor error. Therefore, our framework encapsulates a larger class of approximators including black-box based approximations with the trade-off of *semiglobal practical stability* based on the approximation error  $\epsilon$ .

## 4. Numerical Results

We conduct numerical experiments on a  $n = 5$  degree-of-freedom (DOF) robotic manipulator with constant input delay. All data, models, and experiments are available on [Github \(https://github.com/t2ance/Predictor-Feedback-Control\)](https://github.com/t2ance/Predictor-Feedback-Control).

The dynamics of the 5 DOF robotic manipulator under input delay  $D$  are governed by

$$M(X(t))\ddot{X}(t) + C(X(t), \dot{X}(t))\dot{X}(t) + G(X(t)) = \tau(t - D), \quad t \in [0, \infty), \quad (26)$$

where  $X(t) \in \mathbb{R}^n$ ,  $\dot{X}(t) \in \mathbb{R}^n$ , and  $\ddot{X}(t) \in \mathbb{R}^n$  are the angles, angular velocities, and angular accelerations of the joints. Additionally,  $\tau(t) \in \mathbb{R}^n$  indicates the vector of joint driving torques which is user-controlled. Lastly,  $M(\cdot) \in \mathbb{R}^{n \times n}$ ,  $C(\cdot, \cdot) \in \mathbb{R}^{n \times n}$ , and  $G(\cdot) \in \mathbb{R}^n$  are the mass, Coriolis,



and gravitational matrices, which are symbolically derived using the Euler-Lagrange equations as in Bagheri and Naseradinmousavi (2017). Note that all coefficient matrices have to be recalculated each time, making the numerical approach, which requires repeatedly computing the dynamic, less inefficient. On the other hand, our NeuralOP-based predictor feedback avoids invoking system dynamics and is much more efficient. In this example, we consider the trajectory tracking task of following  $X_{\text{des}} = 0.1[\sin(t), \cos(t), \sin(t), \cos(t), \sin(t)]$  for all  $t \geq 0$  under input delay  $D = 0.5\text{s}$ . To develop the control law, we consider the feedback linearization approach of Bagheri et al. (2019) detailed in Appendix C.1.

Table 1: Performance of various predictor approximation approaches across 25 sampled trajectories. Each trajectory is run for  $T = 8$  seconds with  $dt = 0.02$  and a delay of  $D = 0.5$  seconds. The initial conditions are sampled from  $[X(0), \dot{X}(0)] \in \text{Uniform}(0, 1)^{2n} + [X_{\text{des}}(0), \dot{X}_{\text{des}}(0)]$  which ensures the error system is sampled from a uniform distribution.

Approximation method	Parameters ↓	Training time (minutes) ↓	Training $L_2$ error ( $\times 10^{-4}$ ) ↓	Testing $L_2$ error ( $\times 10^{-4}$ ) ↓	Avg. trajectory $L_2$ error ↓	Avg. trajectory rel. $L_2$ error ↓	Prediction time (ms) ↓
Successive approximations	N/A	N/A	N/A	N/A	$4.614 \times 10^{-10}$	$4.376 \times 10^{-9}$	583.508
GRU	<b>116042</b>	<b>5.531</b>	1.64	1.64	<b>0.046</b>	0.278	1.544
LSTM	154506	9.649	1.42	1.42	0.068	0.303	<b>1.381</b>
FNO	826506	8.291	1.70	1.70	0.212	0.396	2.973
DeepONet	466042	7.897	1.16	1.16	0.076	0.357	2.006
FNO + GRU	1515156	14.245	<b>1.07</b>	<b>1.14</b>	0.092	0.323	5.096
DeepONet + GRU	1062788	8.766	1.15	<b>1.14</b>	0.048	<b>0.272</b>	2.410

For our predictor feedback approximations, we employ a series of approaches including the successive approximation approach in Karafyllis and Krstic (2017), RNNs (GRU (Cho et al., 2014) and LSTM (Hochreiter and Schmidhuber, 1997)), classical neural operators (FNO (Li et al., 2021) and DeepONet (Lu et al., 2021)), and spatio-temporal neural operators (FNO + GRU and DeepONet + GRU (Michałowska et al., 2024)) that combine RNNs and neural operators. To develop a suitable training set for learning, we simulate the robot dynamics collecting trajectory samples of expected prediction and control inputs for various initial conditions (sampled from  $[X(0), \dot{X}(0)] \in \text{Uniform}(0, 1)^{2n} + [X_{\text{des}}(0), \dot{X}_{\text{des}}(0)]$ ) yielding 240,000 total samples to learn from (See Appendix C.2 for all dataset generation and training details). In Table 1, we present the training and testing  $L_2$  errors of each approach. We see that each method is able to achieve an  $L_2$  accuracy on the magnitude of  $10^{-4}$ . Further, to evaluate the neural operator approximated predictors in a feedback controller, we simulate the closed-loop performance of the approximated predictors in 25 trajectories with varying initial conditions sampled in the same way as the training set. For all 25 trajectories, every method stabilizes (despite the less accurate approximation of the NeuralOP approach), and we report the trajectory errors between  $X(t + D)$  and  $\hat{P}(t)$  in Table 1. Note the trajectory errors (second and third last columns in Table 1) are generally larger than the testing errors, since it is online testing that suffers error accumulation and the data does not satisfy the independent and identically distributed (i.i.d.) assumption. In the last column of Table 1, we compare the average prediction time across all approaches (Nvidia 2080Ti) and see that all neural-network based approaches significantly outperform the numerical scheme in terms of computational speed. Lastly, we showcase an example trajectory in Figure 2 comparing the successive approximations approach with the DeepONet+GRU predictor. Despite the coarser approximation of the NeuralOP approach, we see that both methods similarly stabilize to the desired trajectory.

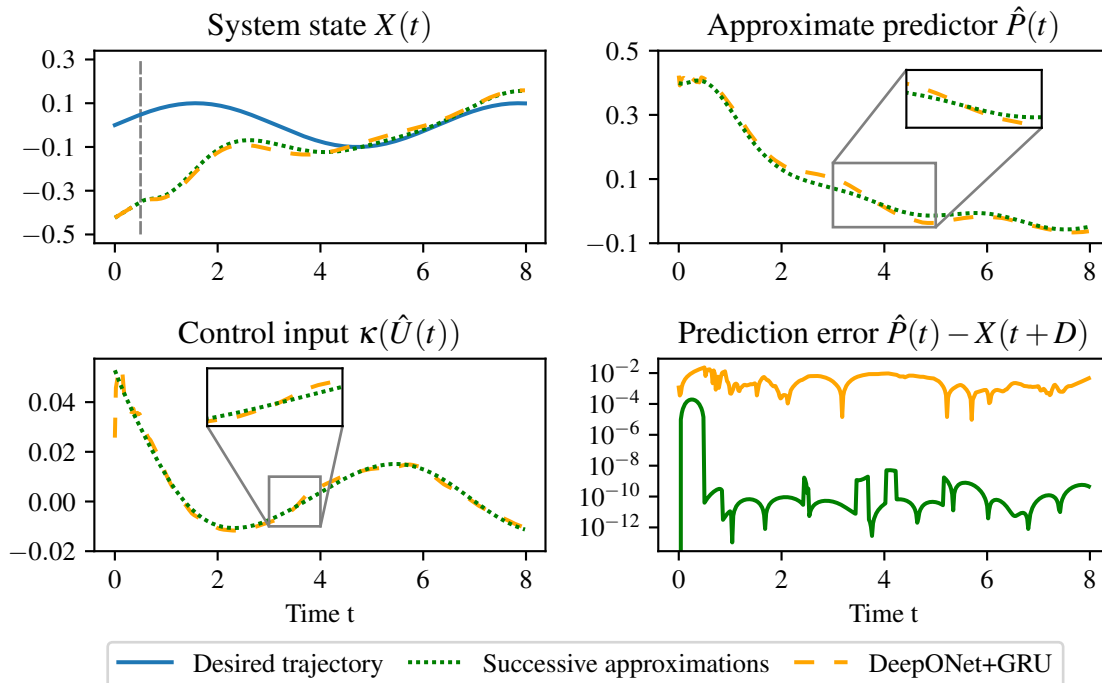


Figure 2: Example of a single trajectory of the robotic manipulator system. The fifth state (the last arm) and the fifth control input are displayed for clarity. The gray line in the top-left figure indicates the arrival of the first control signal at the delay of  $D = 0.5$  seconds. The bottom-right figure shows the prediction error under successive approximation (green line) and DeepONet+GRU (yellow line).

## 5. Conclusion and Future Work

In this work, we developed NeuralOP approximations of predictors and analyzed the resulting stability estimates in nonlinear delay systems. Particularly, (1) we defined the predictor operator and established its continuity enabling the existence of an arbitrary good NeuralOP approximation. Additionally, (2) we presented a semiglobal practical stability estimate whose initial conditions can be made arbitrarily large at the price of a more challenging NeuralOP approximation. This estimate is unique as it can be applied to *any* black-box approximate predictor satisfying a uniform error bound. Lastly, (3) we highlighted the advantage of our approach on a 5-link robotic manipulator attaining speedups on the magnitude of  $10^2$  over the numerical approximated predictor of [Gu et al. \(2003\)](#).

Fundamentally, this is the first work to consider *black-box* approximate predictors with uniform approximation errors. Our final result, Theorem 7, presenting semi-global practical stability for approximate predictors, is the first of its kind with minimal assumptions. It crucially relies on the universal approximation theorem of neural operators and the  $L^\infty$  stability estimate of the transport PDE. Intentionally, this work focused on the simplest possible non-trivial problem - the constant input delay case - for which the analysis is challenging. Thus, by following the blueprint laid out in this work, there is ample opportunity for extensions including non-constant input delays ([Bekiaris-Liberis and Krstic, 2011](#)), distributed input delays ([Bekiaris-Liberis and Krstic, 2016](#)) and delay-adaptive ([Bresch-Pietri and Krstic, 2014](#)) predictor feedback designs.

## References

- Ignacio Abadía, Francisco Naveros, Eduardo Ros, Richard R. Carrillo, and Niceto R. Luque. A cerebellar-based solution to the nondeterministic time delay problem in robotic control. *Science Robotics*, 6(58), 2021. doi: 10.1126/scirobotics.abf2756. URL <https://www.science.org/doi/abs/10.1126/scirobotics.abf2756>.
- Miguel Aguiar, Amritam Das, and Karl H. Johansson. Learning flow functions of spiking systems. In Alessandro Abate, Mark Cannon, Kostas Margellos, and Antonis Papachristodoulou, editors, *Proceedings of the 6th Annual Learning for Dynamics & Control Conference*, volume 242 of *Proceedings of Machine Learning Research*, pages 591–602. PMLR, 15–17 Jul 2024. URL <https://proceedings.mlr.press/v242/aguiar24a.html>.
- Z. Artstein. Linear systems with delayed controls: A reduction. *IEEE Transactions on Automatic Control*, 27(4):869–879, 1982. doi: 10.1109/TAC.1982.1103023.
- Mostafa Bagheri and Peiman Naseradinmousavi. Novel analytical and experimental trajectory optimization of a 7-DOF Baxter robot: global design sensitivity and step size analyses. *The International Journal of Advanced Manufacturing Technology*, 93:4153–4167, 2017.
- Mostafa Bagheri, Peiman Naseradinmousavi, and Miroslav Krstić. Feedback linearization based predictor for time delay control of a high-DOF robot manipulator. *Automatica*, 108:108485, 2019. ISSN 0005-1098. doi: <https://doi.org/10.1016/j.automatica.2019.06.037>. URL <https://www.sciencedirect.com/science/article/pii/S0005109819303371>.
- Georges Bastin, Jean-Michel Coron, and Amaury Hayat. Input-to-state stability in sup norms for hyperbolic systems with boundary disturbances. *Nonlinear Analysis*, 208:112300, 2021. ISSN 0362-546X. doi: <https://doi.org/10.1016/j.na.2021.112300>. URL <https://www.sciencedirect.com/science/article/pii/S0362546X21000389>.
- Nikolaos Bekiaris-Liberis and Miroslav Krstic. Compensation of Time-Varying Input and State Delays for Nonlinear Systems. *Journal of Dynamic Systems, Measurement, and Control*, 134(1): 011009, 12 2011. ISSN 0022-0434. doi: 10.1115/1.4005278. URL <https://doi.org/10.1115/1.4005278>.
- Nikolaos Bekiaris-Liberis and Miroslav Krstic. *Nonlinear Control Under Nonconstant Delays*. Society for Industrial and Applied Mathematics, Philadelphia, PA, 2013. doi: 10.1137/1.9781611972856. URL <https://epubs.siam.org/doi/abs/10.1137/1.9781611972856>.
- Nikolaos Bekiaris-Liberis and Miroslav Krstic. Stability of predictor-based feedback for nonlinear systems with distributed input delay. *Automatica*, 70:195–203, 2016. ISSN 0005-1098. doi: <https://doi.org/10.1016/j.automatica.2016.04.011>. URL <https://www.sciencedirect.com/science/article/pii/S0005109816301339>.
- Nikolaos Bekiaris-Liberis and Miroslav Krstic. Predictor-feedback stabilization of multi-input nonlinear systems. *IEEE Transactions on Automatic Control*, 62(2):516–531, 2017. doi: 10.1109/TAC.2016.2558293.

- Luke Bhan, Yuanyuan Shi, and Miroslav Krstic. Neural operators for bypassing gain and control computations in PDE backstepping. *IEEE Transactions on Automatic Control*, 69(8):5310–5325, 2024. doi: 10.1109/TAC.2023.3347499.
- Luke Bhan, Yuanyuan Shi, and Miroslav Krstic. Adaptive control of reaction–diffusion PDEs via neural operator-approximated gain kernels. *Systems & Control Letters*, 195:105968, 2025. ISSN 0167-6911. doi: <https://doi.org/10.1016/j.sysconle.2024.105968>. URL <https://www.sciencedirect.com/science/article/pii/S0167691124002561>.
- Delphine Bresch-Pietri and Miroslav Krstic. Delay-adaptive control for nonlinear systems. *IEEE Transactions on Automatic Control*, 59(5):1203–1218, 2014. doi: 10.1109/TAC.2014.2298711.
- Filippo Cacace and Alfredo Germani. Output feedback control of linear systems with input, state and output delays by chains of predictors. *Automatica*, 85:455–461, 2017. ISSN 0005-1098. doi: <https://doi.org/10.1016/j.automatica.2017.08.013>. URL <https://www.sciencedirect.com/science/article/pii/S000510981730434X>.
- Ricky T. Q. Chen, Yulia Rubanova, Jesse Bettencourt, and David K Duvenaud. Neural ordinary differential equations. In S. Bengio, H. Wallach, H. Larochelle, K. Grauman, N. Cesa-Bianchi, and R. Garnett, editors, *Advances in Neural Information Processing Systems*, volume 31. Curran Associates, Inc., 2018. URL [https://proceedings.neurips.cc/paper\\_files/paper/2018/file/69386f6bb1dfed68692a24c8686939b9-Paper.pdf](https://proceedings.neurips.cc/paper_files/paper/2018/file/69386f6bb1dfed68692a24c8686939b9-Paper.pdf).
- Yuan Chen and Dongbin Xiu. Learning stochastic dynamical system via flow map operator. *Journal of Computational Physics*, 508:112984, 2024. ISSN 0021-9991. doi: <https://doi.org/10.1016/j.jcp.2024.112984>. URL <https://www.sciencedirect.com/science/article/pii/S002199912400233X>.
- Kyunghyun Cho, Bart van Merriënboer, Dzmitry Bahdanau, and Yoshua Bengio. On the properties of neural machine translation: Encoder–decoder approaches. In Dekai Wu, Marine Carpuat, Xavier Carreras, and Eva Maria Vecchi, editors, *Proceedings of SSST-8, Eighth Workshop on Syntax, Semantics and Structure in Statistical Translation*, pages 103–111, Doha, Qatar, October 2014. Association for Computational Linguistics. doi: 10.3115/v1/W14-4012. URL <https://aclanthology.org/W14-4012>.
- Keqin Gu, Vladimir Kharitonov, L., and Jie Chen. *Stability of Time-Delay Systems*. Birkhäuser Boston, MA, 2003.
- Michael A Henson and Dale E Seborg. Time delay compensation for nonlinear processes. *Industrial & engineering chemistry research*, 33(6):1493–1500, 1994.
- Sepp Hochreiter and Jürgen Schmidhuber. Long short-term memory. *Neural Comput.*, 9(8):1735–1780, November 1997. ISSN 0899-7667. doi: 10.1162/neco.1997.9.8.1735. URL <https://doi.org/10.1162/neco.1997.9.8.1735>.
- M. Jankovic. Control Lyapunov-Razumikhin functions and robust stabilization of time delay systems. *IEEE Transactions on Automatic Control*, 46(7):1048–1060, 2001. doi: 10.1109/9.935057.

- M. Jankovic. Control of nonlinear systems with time delay. In *42nd IEEE International Conference on Decision and Control (IEEE Cat. No.03CH37475)*, volume 5, pages 4545–4550 Vol.5, 2003. doi: 10.1109/CDC.2003.1272267.
- Mrdjan Jankovic. Recursive predictor design for state and output feedback controllers for linear time delay systems. *Automatica*, 46(3):510–517, 2010. ISSN 0005-1098. doi: <https://doi.org/10.1016/j.automatica.2010.01.021>. URL <https://www.sciencedirect.com/science/article/pii/S0005109810000415>.
- Iasson Karafyllis. Finite-time global stabilization by means of time-varying distributed delay feedback. *SIAM Journal on Control and Optimization*, 45(1):320–342, 2006. doi: 10.1137/040616383. URL <https://doi.org/10.1137/040616383>.
- Iasson Karafyllis and Miroslav Krstic. *Predictor Feedback for Delay Systems: Implementations and Approximations*. Birkhäuser Cham, 2017.
- Iasson Karafyllis and Miroslav Krstic. *Input-to-State Stability for PDEs*. Springer Cham, 2018.
- Iasson Karafyllis and Miroslav Krstic. Stability results for the continuity equation. *Systems & Control Letters*, 135:104594, 2020. ISSN 0167-6911. doi: <https://doi.org/10.1016/j.sysconle.2019.104594>. URL <https://www.sciencedirect.com/science/article/pii/S016769111930204X>.
- Nikola Kovachki, Samuel Lanthaler, and Siddhartha Mishra. On universal approximation and error bounds for Fourier neural operators. *J. Mach. Learn. Res.*, 22(1), January 2021. ISSN 1532-4435.
- Costas Kravaris and Raymond A. Wright. Deadtime compensation for nonlinear processes. *AIChE Journal*, 35(9):1535–1542, 1989. doi: <https://doi.org/10.1002/aic.690350914>. URL <https://aiche.onlinelibrary.wiley.com/doi/abs/10.1002/aic.690350914>.
- Miroslav Krstic. Input delay compensation for forward complete and strict-feedforward nonlinear systems. *IEEE Transactions on Automatic Control*, 55(2):287–303, 2010. doi: 10.1109/TAC.2009.2034923.
- Miroslav Krstic, Petar V. Kokotovic, and Ioannis Kanellakopoulos. *Nonlinear and Adaptive Control Design*. John Wiley & Sons, Inc., USA, 1st edition, 1995. ISBN 0471127329.
- W. Kwon and A. Pearson. Feedback stabilization of linear systems with delayed control. *IEEE Transactions on Automatic Control*, 25(2):266–269, 1980. doi: 10.1109/TAC.1980.1102288.
- Maxence Lamarque, Luke Bhan, Yuanyuan Shi, and Miroslav Krstic. Adaptive neural-operator backstepping control of a benchmark hyperbolic PDE, 2024a. URL <https://arxiv.org/abs/2401.07862>.
- Maxence Lamarque, Luke Bhan, Rafael Vazquez, and Miroslav Krstic. Gain scheduling with a neural operator for a transport PDE with nonlinear recirculation, 2024b. URL <https://arxiv.org/abs/2401.02511>.

- Samuel Lanthaler, Siddhartha Mishra, and George E Karniadakis. Error estimates for DeepONets: a deep learning framework in infinite dimensions. *Transactions of Mathematics and Its Applications*, 6(1):tnac001, 03 2022. ISSN 2398-4945. doi: 10.1093/imatrm/tnac001. URL <https://doi.org/10.1093/imatrm/tnac001>.
- Samuel Lanthaler, Zongyi Li, and Andrew M. Stuart. The Nonlocal Neural Operator: Universal Approximation, 2023. arXiv preprint; <https://arxiv.org/abs/2304.13221>.
- Zongyi Li, Nikola Borislavov Kovachki, Kamyar Azizzadenesheli, Burigede liu, Kaushik Bhattacharya, Andrew Stuart, and Anima Anandkumar. Fourier neural operator for parametric partial differential equations. In *International Conference on Learning Representations*, 2021. URL <https://openreview.net/forum?id=c8P9NQVtmnO>.
- Ilya Loshchilov and Frank Hutter. Decoupled weight decay regularization. In *International Conference on Learning Representations*, 2019. URL <https://openreview.net/forum?id=Bkg6RiCqY7>.
- Lu Lu, Pengzhan Jin, Guofei Pang, Zhongqiang Zhang, and George Em Karniadakis. Learning nonlinear operators via DeepONet based on the universal approximation theorem of operators. *Nature Machine Intelligence*, 3(3):218–229, Mar 2021. ISSN 2522-5839. doi: 10.1038/s42256-021-00302-5. URL <https://doi.org/10.1038/s42256-021-00302-5>.
- Mitchell J.H. Lum, Jacob Rosen, Hawkeye King, Diana C.W. Friedman, Thomas S. Lendvay, Andrew S. Wright, Mika N. Sinanan, and Blake Hannaford. Teleoperation in surgical robotics – network latency effects on surgical performance. In *2009 Annual International Conference of the IEEE Engineering in Medicine and Biology Society*, pages 6860–6863, 2009. doi: 10.1109/IEMBS.2009.5333120.
- Kaijing Lv, Junmin Wang, Yihuai Zhang, and Huan Yu. Neural operators for adaptive control of freeway traffic, 2024. URL <https://arxiv.org/abs/2410.20708>.
- Sindri Magnússon, Guannan Qu, and Na Li. Distributed optimal voltage control with asynchronous and delayed communication. *IEEE Transactions on Smart Grid*, 11(4):3469–3482, 2020.
- F. Mazenc and P.-A. Bliman. Backstepping design for time-delay nonlinear systems. In *42nd IEEE International Conference on Decision and Control (IEEE Cat. No.03CH37475)*, volume 5, pages 4551–4556 Vol.5, 2003. doi: 10.1109/CDC.2003.1272269.
- Frédéric Mazenc, Michael Malisoff, Corina Barbalata, and Zhong-Ping Jiang. Subpredictor approach for event-triggered control of discrete-time systems with input delays. *European Journal of Control*, 68:100664, 2022. ISSN 0947-3580. doi: <https://doi.org/10.1016/j.ejcon.2022.100664>. URL <https://www.sciencedirect.com/science/article/pii/S094735802000565>. 2022 European Control Conference Special Issue.
- Katarzyna Michałowska, Somdatta Goswami, George Em Karniadakis, and Signe Riemers-Sørensen. Neural operator learning for long-time integration in dynamical systems with recurrent neural networks, 2024. URL <https://arxiv.org/abs/2303.02243>.

Jie Qi, Jing Zhang, and Miroslav Krstic. Neural operators for PDE backstepping control of first-order hyperbolic PIDE with recycle and delay. *Systems & Control Letters*, 185:105714, 2024. ISSN 0167-6911. doi: <https://doi.org/10.1016/j.sysconle.2024.105714>. URL <https://www.sciencedirect.com/science/article/pii/S0167691124000021>.

Nitin Sharma, Chris M Gregory, and Warren E Dixon. Predictor-based compensation for electromechanical delay during neuromuscular electrical stimulation. *IEEE Trans. Neural Syst. Rehabil. Eng.*, 19(6):601–611, December 2011.

Otto JM Smith. Closer control of loops with dead time. *Chemical engineering progress*, 53:217–219, 1957.

E.D. Sontag and Yuan Wang. New characterizations of input-to-state stability. *IEEE Transactions on Automatic Control*, 41(9):1283–1294, 1996. doi: 10.1109/9.536498.

Jianan Wang, Zhengyang Zhou, Chunyan Wang, and Zhengtao Ding. Cascade structure predictive observer design for consensus control with applications to uavs formation flying. *Automatica*, 121:109200, 2020. ISSN 0005-1098. doi: <https://doi.org/10.1016/j.automatica.2020.109200>. URL <https://www.sciencedirect.com/science/article/pii/S0005109820303988>.

Yihuai Zhang, Ruiguo Zhong, and Huan Yu. Neural operators for boundary stabilization of stop-and-go traffic. In Alessandro Abate, Mark Cannon, Kostas Margellos, and Antonis Papachristodoulou, editors, *Proceedings of the 6th Annual Learning for Dynamics & Control Conference*, volume 242 of *Proceedings of Machine Learning Research*, pages 554–565. PMLR, 15–17 Jul 2024. URL <https://proceedings.mlr.press/v242/zhang24c.html>.

Bin Zhou. *Truncated Predictor Feedback for Time-Delay Systems*. Springer Berlin, Heidelberg, 2014.

## Appendix A. Technical Background

### A.1. Strongly-forward complete

**Definition 8** (*Krstic, 2010, Definition 6.1*) *The system  $\dot{X} = f(X, \omega)$  with  $f(0, 0) = 0$  is strongly forward complete if there exists a smooth function  $R : \mathbb{R}^n \rightarrow [0, \infty)$  and class  $\mathcal{K}_\infty$  functions,  $\alpha_1, \alpha_2, \alpha_3$  such that*

$$\alpha_1(|X|) \leq R(X) \leq \alpha_2(|X|), \quad (27)$$

$$\frac{\partial R(X)}{\partial X} f(X, \omega) \leq R(X) + \alpha_3(|\omega|), \quad (28)$$

for all  $X \in \mathbb{R}^n$  and for all  $\omega \in \mathbb{R}^m$ .

### A.2. Input-to-state stability (ISS)

**Definition 9** (*Sontag and Wang, 1996*) *The system  $\dot{X} = f(X, \kappa(X) + \omega)$  is input-to-state stable (ISS) if there exists a class  $\mathcal{KL}$  function  $\beta$  and a class  $\mathcal{K}$  function  $\sigma$ , such that for any  $X(0)$ , and for any continuous, bounded input  $\omega(\cdot)$ , the solution exists for all  $t \geq 0$  and satisfies*

$$|X(t)| \leq \beta(|X(t_0)|, t - t_0) + \sigma \left( \sup_{t_0 \leq \tau \leq t} |\omega(\tau)| \right), \quad (29)$$

for all  $t_0, t$  such that  $0 \leq t_0 \leq t$ .

### A.3. Review of neural operators

For convenience, we provide a small overview of neural operators. In essence, neural operators aim to use neural network architectures to approximate *operator* mappings with the goal of improved scalability and discretization invariance. To begin, we review the Nonlocal Neural Operator (NNO) (*Lanthaler et al., 2023*) - a framework that encompasses a majority of the popular architectures, including DeepONet and FNO.

Let  $\Omega_u \subset \mathbb{R}^{d_{u1}}$ ,  $\Omega_v \subset \mathbb{R}^{d_{v1}}$  be bounded domains and define the following function spaces consisting of continuous functions  $\mathcal{F}_c \subset C^0(\Omega_u; \mathbb{R}^c)$ ,  $\mathcal{F}_v \subset C^0(\Omega_v; \mathbb{R}^v)$ . Then, a NNO is defined as a mapping  $\hat{\Psi} : \mathcal{F}_c(\Omega_u; \mathbb{R}^c) \rightarrow \mathcal{F}_v(\Omega_v; \mathbb{R}^v)$  which can be written in the compositional form  $\hat{\Psi} = \mathcal{Q} \circ \mathcal{L}_L \circ \dots \circ \mathcal{L}_1 \circ \mathcal{R}$  consisting of a lifting layer  $\mathcal{R}$ , hidden layers  $\mathcal{L}_l, l = 1, \dots, L$ , and a projection layer  $\mathcal{Q}$ . Given a channel dimension  $d_c$ , the lifting layer  $\mathcal{R}$  is given by

$$\mathcal{R} : \mathcal{F}_c(\Omega_u; \mathbb{R}^c) \rightarrow \mathcal{F}_s(\Omega_s; \mathbb{R}^{d_c}), \quad c(x) \mapsto R(c(x), x), \quad (30)$$

where  $\Omega_s \subset \mathbb{R}^{d_{s1}}$ ,  $\mathcal{F}_s(\Omega_s; \mathbb{R}^{d_c})$  is a Banach space for the hidden layers and  $R : \mathbb{R}^c \times \Omega_u \rightarrow \mathbb{R}^{d_c}$  is a learnable neural network acting between finite-dimensional Euclidean spaces. For  $l = 1, \dots, L$  each hidden layer  $\mathcal{L}_l$  is of the form

$$(\mathcal{L}_l v)(x) := \sigma(W_l v(x) + b_l + (\mathcal{K}_l v)(x)) \quad (31)$$

where weights  $W_l \in \mathbb{R}^{d_c \times d_c}$  and biases  $b_l \in \mathbb{R}^{d_c}$  are learnable parameters,  $\sigma : \mathbb{R} \rightarrow \mathbb{R}$  is a smooth, infinitely differentiable activation function that acts component wise on inputs and  $\mathcal{K}_l$  is the nonlocal operator given by

$$(\mathcal{K}_l v)(x) = \int_{\mathcal{X}} K_l(x, y) v(y) dy \quad (32)$$

where  $K_l(x, y)$  is the kernel containing learnable parameters given in various forms. For example, in the FNO (*Li et al., 2021*) architecture,  $K_l(x, y) = K_l(x - y)$ ,  $K_l(x) = \sum_{|k| \leq k_{\max}} \hat{P}_{l,k} e^{ikx}$  is a trigonometric polynomial (Fourier) approximation with  $k_{\max}$  nodes and  $\hat{P}_{l,k}$  is a matrix of complex, learnable parameters  $\hat{P}_{l,k} \in \mathbb{C}^{d_c \times d_c}$ . Note that (31) is almost a traditional feed-forward neural network except for the kernel term (32), which is nonlocal - it depends on points over the entire domain rather than just  $x$ . Lastly, the projection layer  $\mathcal{Q}$  is defined as

$$\mathcal{Q} : \mathcal{F}_s(\Omega_s; \mathbb{R}^{d_c}) \rightarrow \mathcal{F}_v(\Omega_v; \mathbb{R}^v), \quad s(x) \mapsto Q(s(x), y), \quad (33)$$

where  $Q$  is a finite dimensional neural network from  $\mathbb{R}^{d_c} \times \Omega_v \rightarrow \mathbb{R}^v$  yielding the final value of the operator ( $\hat{\Psi}c$ ) ( $c \in \mathcal{F}_c$ ) at the point  $x \in \Omega_v$ .



#### A.4. Universal operator approximation theorem

**Theorem 10** (*Lanthaler et al., 2023, Theorem 2.1*) *Let  $\Omega_u \subset \mathbb{R}^{d_{u_1}}$  and  $\Omega_v \subset \mathbb{R}^{d_{v_1}}$  be two bounded domains with Lipschitz boundary. Let  $\mathcal{G} : C^0(\overline{\Omega_u}; \mathbb{R}^{d_{u_2}}) \rightarrow C^0(\overline{\Omega_v}; \mathbb{R}^{d_{v_2}})$  be a continuous operator and fix a compact set  $K \subset C^0(\overline{\Omega_u}; \mathbb{R}^{d_{u_2}})$ . Then for any  $\epsilon > 0$ , there exists a neural operator  $\hat{\mathcal{G}} : K \rightarrow C^0(\overline{\Omega_v}; \mathbb{R}^{d_{v_2}})$  such that*

$$\sup_{u \in K} |\mathcal{G}(u)(y) - \hat{\mathcal{G}}(u)(y)| \leq \epsilon, \quad (34)$$

for all values  $y \in \Omega_v$ .

### Appendix B. Proofs of technical results

#### B.1. Proof of Lemma 3

For all  $s \in [-D, 0]$ , let  $P_1(s) := \mathcal{P}(X_1, U_1)(s)$  and likewise  $P_2(s) := \mathcal{P}(X_2, U_2)(s)$ . Then, we have

$$\begin{aligned} P_1(s) - P_2(s) &= X_1 - X_2 + \int_{-D}^s f(P_1(\theta), U_1(\theta)) - f(P_2(\theta), U_2(\theta)) d\theta \\ &\leq |X_1 - X_2| + \int_{-D}^s C_f (|P_1(\theta) - P_2(\theta)| + |U_1(\theta) - U_2(\theta)|) d\theta \\ &\leq |X_1 - X_2| + DC_f \|U_1 - U_2\|_{L^\infty([-D, s])} + \int_{-D}^s C_f (|P_1(\theta) - P_2(\theta)|) d\theta \\ &\leq \exp(DC_f) (|X_1 - X_2| + DC_f (\|U_1 - U_2\|_{L^\infty([-D, s])})), \end{aligned} \quad (35)$$

where we used the definition of the predictor, Lipschitz continuity in Assumption 4, properties of the  $L^\infty$  norm in the integral, and Gronwall's inequality. Now, noting that the bound is monotonically increasing with respect to  $s$ , we can take  $s \rightarrow 0$  to yield the result.

#### B.2. Proof of Theorem 4

Note that  $\mathcal{X}$  and  $\mathcal{U}$  are both bounded domains. Further, from Lemma 3, the operator  $\mathcal{P}$  is continuous. Thus, we apply Theorem 10 to achieve the result.

#### B.3. Proof of Lemma 5

The PDE representation of the system with the approximate predictor is as follows

$$\dot{X}(t) = f(X(t), u(t, 0)), \quad t \in [0, \infty) \quad (36)$$

$$u_t(x, t) = u_x(x, t), \quad (x, t) \in [0, D) \times [0, \infty), \quad (37)$$

$$u(D, t) = \kappa(\hat{P}(t)), \quad t \in [0, \infty). \quad (38)$$

Under the transform with the exact predictor, namely

$$w(x, t) = u(x, t) - \kappa(p(x, t)) \quad (39)$$

we have

$$w_t = u_t - \frac{\partial}{\partial t} k(p(x, t)) \quad (40)$$

$$w_x = u_x - \frac{\partial}{\partial x} k(p(x, t)) \quad (41)$$

Noting, that  $u_t = u_x$  and noting that the function  $p(x, t)$  is really a function of only one variable, namely  $x + t$  as it is the solution to the ODE (8), yields  $w_t = w_x$ . Substituting the boundary conditions at  $x = D$  into (39) and noting  $u(D, t) = \kappa(\hat{P}(t))$  yields (20c).

#### B.4. Proof of Lemma 6

As standard with transport PDEs, we aim to analyze the exponentially weighted norm of the form

$$\|w(t)\|_{c,\infty} = \sup_{x \in [0, D]} |e^{cx} w(x, t)| = \lim_{p \rightarrow \infty} \left( \int_0^D e^{pcx} |w(x, t)|^p dx \right)^{\frac{1}{p}}, \quad (42)$$

where  $c > 0$  which we note satisfies

$$\|w(t)\|_{L^\infty[0, D]} \leq \|w(t)\|_{c, L^\infty[0, D]} \leq e^{cD} \|w(t)\|_{L^\infty[0, D]}. \quad (43)$$

Thus, we will begin by analyzing the Lyapunov functional of  $L^p$  norm, namely for  $p \in (1, \infty)$ , we have

$$V(t) = \|w(t)\|_{c,p}^p. \quad (44)$$

Taking the derivative, substitution of  $w_t = w_x$  and applying integration by parts yields

$$\begin{aligned} \dot{V}(t) &= p \int_0^D e^{pcx} \operatorname{sgn}(w(x, t)) |w(x, t)|^{p-1} w_t(x, t) dx, && \text{Differentiation} \\ &= p \int_0^D e^{pcx} \operatorname{sgn}(w(x, t)) |w(x, t)|^{p-1} w_x(x, t) dx, && \text{Substitution } w_t = w_x \\ &= e^{pcD} |w(D, t)|^p - pc \int_0^D e^{pcx} |w(x, t)|^p dx, && \text{Integration by parts} \\ &= e^{pcD} |w(D, t)|^p - |w(0, t)|^p - pcV, && \text{Substitution of } V \\ &\leq e^{pcD} |w(D, t)|^p - pcV. && \text{Properties of inequality} \end{aligned} \quad (45)$$

From (45), we obtain

$$V(t) \leq V(0) e^{-pct} + \frac{e^{pcD}}{pc} \sup_{0 \leq \tau \leq t} |w(D, \tau)|^p. \quad (46)$$

Now, substituting  $V(t)$  into (42) and noting that  $\lim_{p \rightarrow \infty} \|w(0)\|_{c, L^p[0, D]} = \|w(0)\|_{c, L^\infty[0, D]}$  yields

$$\begin{aligned} \|w(t)\|_{c,\infty} &= \lim_{p \rightarrow \infty} (V(t))^{\frac{1}{p}} \\ &\leq \lim_{p \rightarrow \infty} \left( \|w(0)\|_{c, L^p[0, D]} e^{-ct} + e^{cD} \left( \frac{1}{cp} \right)^{\frac{1}{p}} \sup_{0 \leq \tau \leq t} |w(D, \tau)| \right) \\ &\leq \|w(0)\|_{c, L^\infty[0, D]} e^{-ct} + e^{cD} \sup_{0 \leq \tau \leq t} |w(D, \tau)| \end{aligned} \quad (47)$$

Noting that the weighted norm satisfies

$$\begin{aligned}
 \|w(t)\|_{L^\infty[0,D]} &\leq \|w(t)\|_{c,L^\infty[0,D]} \\
 &\leq \|w_0\|_{c,L^\infty[0,D]} e^{-ct} + e^{cD} \sup_{0 \leq \tau \leq t} |w(D, \tau)| \\
 &\leq \|w_0\|_{L^\infty[0,D]} e^{c(D-t)} + e^{cD} \sup_{0 \leq \tau \leq t} |w(D, \tau)|, \tag{48}
 \end{aligned}$$

yields the final result.

The reader familiar with ISS estimates will note that this estimate is not of the typical form in that we do not explicitly achieve a bound on  $\frac{d\|w(t)\|_{c,\infty}}{dt}$  and invoke the comparison Lemma directly. Instead, we achieve such a result on  $\|w(t)\|_{c,p}^p$  and take the limit. This approach is common in supremum norm estimates of the transport PDE (Karafyllis and Krstic, 2020, 2018; Bastin et al., 2021) and the main advantage over Krstic (2010) is avoiding the complications with negative exponents which are undefined at  $w(t) \equiv 0$ .

### B.5. Proof of Theorem 7

We begin by bounding the function  $|X(t)| + \|w(t)\|_{L^\infty[0,D]}$ . First, applying Assumption 2, we know there exists class  $\mathcal{K}_\infty$  functions  $\alpha_2, \alpha_3, \alpha_4, \alpha_5$  such that

$$\alpha_2(|X(t)|) \leq S(X(t)) \leq \alpha_3(|X(t)|), \tag{49}$$

$$\frac{\partial S(X(t))}{\partial Z} f(X(t), \kappa(X(t)) + w(0, t)) \leq -\alpha_4(|X(t)|) + \alpha_5(|w(0, t)|). \tag{50}$$

Now, we first bound  $|X(t)|$ . We begin by defining the Lyapunov function

$$\check{V}(t) = S(X(t)), \tag{51}$$

as in (49). Then, we have that

$$\begin{aligned}
 \dot{\check{V}} &\leq -\alpha_4(|X(t)|) + \alpha_5(|w(0, t)|) \\
 &\leq -\alpha_4(|X(t)|) + \alpha_5 \left( \sup_{0 \leq x \leq D} |w(x, t)| \right) \\
 &= -\alpha_4(|X(t)|) + \alpha_5 (\|w(t)\|_{L^\infty[0,D]}) \\
 &\leq -\alpha_4(|X(t)|) + \alpha_5 \left( \|w(0)\|_{L^\infty[0,D]} e^{c(D-t)} + e^{cD} \sup_{0 \leq \tau \leq t} |w(D, \tau)| \right), \tag{52}
 \end{aligned}$$

where in the last inequality, we applied the stability bound in Lemma 6. Reproducing the argument from Krstic et al. (1995, Lemma C.4), we have that there exists  $\beta_3 \in \mathcal{KL}$ ,  $\alpha_7 \in \mathcal{K}_\infty$  such that

$$\check{V}(t) \leq \beta_3(|X(0)|, t) + \alpha_7 \left( \|w(0)\|_{L^\infty[0,D]} e^{c(D-t)} + e^{cD} \sup_{0 \leq \tau \leq t} |w(D, \tau)| \right). \tag{53}$$

Now applying (49), we have, there exists  $\beta_4 \in \mathcal{KL}$ ,  $\alpha_8 \in \mathcal{K}_\infty$  such that

$$|X(t)| \leq \beta_4(|X(0)|, t) + \alpha_8 \left( \|w(0)\|_{L^\infty[0,D]} e^{c(D-t)} + e^{cD} \sup_{0 \leq \tau \leq t} |w(D, \tau)| \right). \tag{54}$$

Now, using the triangle inequality for class  $\mathcal{K}$  functions, ( $\alpha_8(x + y) \leq \alpha_8(2x) + \alpha_8(2y)$ ), we have that

$$|X(t)| \leq \beta_4(|X(0)|, t) + \alpha_8 \left( 2\|w(0)\|_{L^\infty[0,D]} e^{c(D-t)} \right) + \alpha_8 \left( 2e^{cD} \sup_{0 \leq \tau \leq t} |w(D, \tau)| \right). \quad (55)$$

It is clear that the middle term is decreasing with respect  $t$  and thus, we have that there exists some function  $\beta_5 \in \mathcal{KL}$  such that

$$|X(t)| \leq \beta_5 \left( |X(0)| + \|w(0)\|_{L^\infty[0,D]}, t \right) + \alpha_8 \left( 2e^{cD} \sup_{0 \leq \tau \leq t} |w(D, \tau)| \right). \quad (56)$$

Now, combining the estimate (56) with the estimate on  $w$  in Lemma 6, we have

$$\begin{aligned} |X(t)| + \|w(t)\|_{L^\infty[0,D]} &\leq \beta_5 \left( |X(0)| + \|w(0)\|_{L^\infty[0,D]}, t \right) + \alpha_8 \left( 2e^{cD} \sup_{0 \leq \tau \leq t} |w(D, \tau)| \right) \\ &\quad + \|w(0)\|_{L^\infty[0,D]} e^{c(D-t)} + e^{cD} \sup_{0 \leq \tau \leq t} |w(D, \tau)|, \end{aligned} \quad (57)$$

Note that (57) implies the existence of  $\beta_6 \in \mathcal{KL}$  and  $\alpha_9 \in \mathcal{K}$  such that

$$|X(t)| + \|w(t)\|_{L^\infty[0,D]} \leq \beta_6 \left( |X(0)| + \|w(0)\|_{L^\infty[0,D]}, t \right) + \alpha_9 \left( \sup_{0 \leq \tau \leq t} |w(D, \tau)| \right). \quad (58)$$

Lastly, we substitute in for  $\sup_{0 \leq \tau \leq t} |w(D, \tau)|$  yielding

$$|X(t)| + \|w(t)\|_{L^\infty[0,D]} \leq \beta_6 \left( |X(0)| + \|w(0)\|_{L^\infty[0,D]}, t \right) + \alpha_9 \left( \sup_{0 \leq \tau \leq t} |\kappa(P(t)) - \kappa(\hat{P}(t))| \right). \quad (59)$$

To complete the proof, notice we used the exact backstepping transformation in (9), (10) and thus can reapply the following two technical Lemmas from Krstic (2010)

**Lemma 11** (Krstic, 2010, Lemma 8) *Let (8) satisfy Assumption 1 and consider (9) as its output map. Then, there exists  $\alpha_{10} \in \mathcal{K}_\infty$  such that*

$$|X(t)| + \|w(t)\|_{L^\infty[0,D]} \leq \alpha_{10} \left( |X(t)| + \|u(t)\|_{L^\infty[0,D]} \right). \quad (60)$$

**Lemma 12** (Krstic, 2010, Lemma 9) *Let (11) satisfy Assumption 2 and consider (10) as its output map. Then there exists  $\alpha_{11} \in \mathcal{K}_\infty$  such that*

$$|X(t)| + \|u(t)\|_{L^\infty[0,D]} \leq \alpha_{11} \left( |X(t)| + \|w(t)\|_{L^\infty[0,D]} \right). \quad (61)$$

Combining Lemma 11, Lemma, 12 and (59) yields

$$\begin{aligned} |X(t)| + \|u(t)\|_{L^\infty[0,D]} &\leq \alpha_{11} \left( |X(t)| + \|w(t)\|_{L^\infty[0,D]} \right) \\ &\leq \alpha_{11} \left( \beta_6 \left( |X(0)| + \|w(0)\|_{L^\infty[0,D]}, t \right) + \alpha_9 \left( \sup_{0 \leq \tau \leq t} |\kappa(P(t)) - \kappa(\hat{P}(t))| \right) \right) \\ &\leq \alpha_{11} \left( \beta_6 \left( \alpha_{10} \left( |X(0)| + \|u(0)\|_{L^\infty[0,D]} \right), t \right) \right. \\ &\quad \left. + \alpha_9 \left( \sup_{0 \leq \tau \leq t} |\kappa(P(t)) - \kappa(\hat{P}(t))| \right) \right), \end{aligned} \quad (62)$$

Applying properties of class  $\mathcal{K}$  functions implies the existence of  $\beta_2 \in \mathcal{KL}$ , and  $\alpha_{12} \in \mathcal{K}_\infty$  such that

$$|X(t)| + \|u(t)\|_{L^\infty[0,D]} \leq \beta_2(|X(0)| + \|u(0)\|_{L^\infty[0,D]}, t) + \alpha_{12} \left( \sup_{0 \leq s \leq t} |\kappa(P(t)) - \kappa(\hat{P}(t))| \right). \quad (63)$$

Now, noting that  $\kappa$  is continuous (Assumption 3), there exists a class  $\mathcal{K}_\infty$  function  $\alpha_{13}$  such that  $\sup_{0 \leq s \leq t} |\kappa(P(t)) - \kappa(\hat{P}(t))| \leq \alpha_{13}(\epsilon)$  where  $\epsilon$  is as in Theorem 4. The result then follows by letting  $\alpha_1 = \alpha_{12} \circ \alpha_{13}$  and returning back to ODE notation.

## Appendix C. Experimental details

### C.1. Derivation of feedback controller for robotic manipulators

Consider the 5-link robot manipulator with the mathematical modeling given in (Bagheri et al., 2019)

$$M(X)\ddot{X} + C(X, \dot{X})\dot{X} + G(X) = \tau, \quad (64)$$

where  $X \in \mathbb{R}^5$ ,  $\dot{X} \in \mathbb{R}^5$ , and  $\ddot{X} \in \mathbb{R}^5$  are the angles, angular velocities, and angular accelerations of the joints.  $\tau \in \mathbb{R}^5$  indicates the vector of joint driving torques which is user controlled. Lastly,  $M(X) \in \mathbb{R}^{5 \times 5}$ ,  $C(X, \dot{X}) \in \mathbb{R}^{5 \times 5}$ , and  $G(X) \in \mathbb{R}^5$  are the mass, Coriolis, and gravitational matrices which are symbolically derived using the Euler-Lagrange equations (Bagheri and Naseradinmousavi, 2017). The multi-input nonlinear system (26) can be written as 10<sup>th</sup>-order ODE with the following general state-space form,

$$\dot{\check{X}} = f_0(\check{X}, U), \quad (65)$$

where  $\check{X} = [X_1, \dots, X_5, \dot{X}_1, \dots, \dot{X}_5]^T \in \mathbb{R}^{10}$  is the vector of states and  $U = \tau \in \mathbb{R}^5$  is the input of nonlinear system (65). Since we are working on the trajectory tracking task of following  $X_{\text{des}} \in \mathbb{R}^5$ , we consider the error dynamics of the form

$$\dot{E} = f(E, U), \quad (66)$$

where  $E = [e_1, e_2]^T \in \mathbb{R}^{10}$  is the vector of error states defined by

$$e_1 = X_{\text{des}} - X, \quad (67)$$

$$e_2 = \dot{e}_1 + \alpha e_1, \quad (68)$$

where  $\alpha \in \mathbb{R}^{7 \times 7}$  is a constant positive definite matrix. Then, following Bagheri et al. (2019), the error dynamics become

$$\begin{bmatrix} \dot{e}_1 \\ \dot{e}_2 \end{bmatrix} = \begin{bmatrix} e_2 - \alpha e_1 \\ \alpha e_2 + h - M^{-1}\tau \end{bmatrix}, \quad (69)$$

where  $h = \ddot{X}_{\text{des}} - \alpha^2 e_1 + M^{-1}(C\dot{X}_{\text{des}} + G + C\alpha e_1 - Ce_2)$ . The feedback linearization based control law  $\tau$  is derived as

$$\tau = \kappa(E) = M(h + (\beta + \alpha)e_2), \quad (70)$$

with  $\beta \in \mathbb{R}^{5 \times 5}$  is any positive definite matrix. We refer the readers to Bagheri et al. (2019) for more details.

**C.2. Experimental settings and hyperparameters**

**Manipulator parameters:**

Following the system dynamics and control law in Appendix C.1, we set  $\alpha = \beta = I_5$ , where  $I$  is the identity matrix. We use the Denavit-Hartenberg parameters for simulation as in Bagheri et al. (2019) and choose to follow the trajectory  $q_{des} = 0.1 \times [\sin(t), \cos(t), \sin(t), \cos(t), \sin(t)]^T$ .

**Parameters for training of learning based predictors:**

For data generation, we present all of the data generation parameters in Table 2. We use the successive approximation solved to a tolerance of  $1 \times 10^{-7}$  for generating the ground truth data which we parallelize across 10 CPU threads taking approximately 3 hours. We summarize all of the hyperparameter settings for training the neural operators in Table 3. Additionally, all of the code, models and datasets are available on Github (<https://github.com/t2ance/Predictor-Feedback-Control>).

Table 2: Data generation settings for creating the training and testing datasets.

Dataset Generation	
Trajectories	600
Samples per trajectory	400
Total samples	240000
Temporal discretization (seconds)	0.02
Delay (seconds)	0.5
Initial condition sampling	$[\ddot{X}(0), \dot{X}(0)] \in \text{Uniform}(0, 1)^{2n} + [X_{des}, \dot{X}_{des}]$
Trajectory length (seconds)	8

Table 3: Model and training settings. The optimizer AdamW is from Loshchilov and Hutter (2019).

	Optimizer	Learning rate scheduler	Number of epochs	Learning rate ( $\times 10^{-3}$ )	Weight decay	Batch size
GRU	AdamW	Exponential (decay by 0.98 each epoch)	100	9.5	$5 \times 10^{-6}$	2048
LSTM				9	$8.5 \times 10^{-4}$	
FNO				7.8	$1.2 \times 10^{-5}$	
DeepONet				3	$1.5 \times 10^{-2}$	
FNO+GRU				6	$2 \times 10^{-4}$	
DeepONet+GRU				0.62	$8 \times 10^{-2}$	